

VERIFICATION OF SHADOW REGION EFFECT ON RADAR CROSS SECTION OF TARGETS USING PHYSICAL OPTICS METHOD

H. El-Ocla

Department of Computer Science
Lakehead University
955 Oliver Road, Thunder Bay, Ontario, Canada P7B 5E1

M. Tateiba

Ariake National College of Technology
Japan

Abstract—Our method that uses current generator operator assumes the current on the entire surface of conducting scatterers. While, Physical Optics (PO) method assumes that the surface current generates only on the illumination region. The effect of the shadow region on the scattering waves is, therefore, proved by comparing our exact method with PO method. In this regard, radar cross-section (RCS) is calculated for smooth concave-convex contour. We work on numerical calculation of the RCS and analyze its characteristics with different target configurations including complexity and size. Concave illumination region is postulated with considering targets are taking large sizes of about five wavelengths. Here, we assume waves propagation and scattering from targets in free space and horizontal polarization (E-wave incidence).

1. INTRODUCTION

Radar cross section (RCS) is a key parameter used in radar design, target detection, and system benchmarks [1–3]. Defined as a far-field parameter it represents the effective target area as seen by a radar, independent of range. Various radar problems require an understanding of this parameter at distances less than infinity. Several methods were introduced to calculate RCS such as Finite Element Method (FEM) [4] and Method of Moment [5]. Despite the high computational accuracy of these methods, they require so long

computational time and so large memory that it is hard to apply in scattering analysis for large size objects like in this paper. Fast Multipole Method (FMM) [6] was proposed to reduce the processing time but yet not enough for large and complex targets.

In earlier work, the problem of scattering waves from conducting targets was solved efficiently via an exact method that uses a current generator operator to calculate the electromagnetic field on the whole surface of the target; actually there are several articles that describe this method, e.g., [7–10], where other references are available. In those studies, numerical results were presented for RCS and backscattering enhancement; our results are in excellent agreement with those conducted for circular cylinder in [11]. The scatterer need not be a simple mathematically defined body. High frequency scattering from, or propagation along, a perfectly conducting boundary with smooth concave–convex surface profile is of interest for a variety of applications as in [12]. We considered a perfectly conducting target with an analytic concave–convex boundary shape. Generated numerical results revealed characteristics that exist with partially convex cross sections and absent with typical convex surface such as circular and elliptic shapes [13].

Wave scattering was found to vary remarkably with many parameters including illumination region curvature, incident wave polarization, and target configuration. When a concave surface is illuminated by a plane wave incidence, the scattering wave may undergo focusing, which is absent when the surface and/or illuminated area of the surface is convex. Focusing and defocusing of scattering waves play a role when the scatterer has a smoothly deformed contour comprising concave and convex portions. Detailed studies of these phenomena were undertaken for partially convex targets with inflection points [8]. However, those studies were limited to the case where the normalized target size is in the range of one wavelength of incident waves in free space. These features appeared to be related to the contributions from shadow region as well as stationary points that spread over the illuminated concave region. Some studies were presented showing the stationary points and creeping waves effects on the scattering waves as in [9, 14, 15]. In this work, we probe the impact of normalized target size together with the prescribed effects on the scattering waves in the far-field response. In this regard, we consider targets are extended to take large sizes up to five wavelengths with concave illumination region. To verify our results, we use physical optics PO method that estimates the scattering fields from the specular region only [16–19]. The extended physical optics (EPO) method was originated by Adachi [20]. A characteristic feature of this method,

in comparison with the conventional physical optics (PO) method, is that the EPO current is assumed over the entire surface of the conducting target, while the PO method assumes the current only on the illuminated surface. As a result, the EPO method was found to be valid in the Rayleigh region and in the resonance region of the scattering, while the PO method is valid in the limit of high frequency. In this sense the EPO method is quite different from the PO method in principle [21]. Accordingly, we would be able to show the effect of shadow region on the backscattering waves in the limit of high frequency using the PO method. We take into our account the horizontal polarization (E-wave incidence). The time factor $\exp(-i\omega t)$ is assumed and suppressed in the following section.

2. SCATTERING PROBLEM

Let us consider scattering waves from targets in free space. Geometry of the problem is shown in Figure 1.

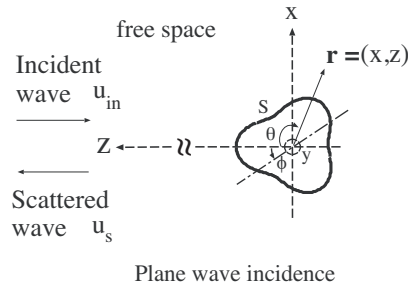


Figure 1. Geometry of the problem of wave scattering from a conducting cylinder.

Here, $k = \omega\sqrt{\epsilon_0\mu_0}$ is the wavenumber in free space.

An electromagnetic wave radiated from a source located at \mathbf{r}_t , that is beyond the target at the far field, propagates in free space, illuminates the target and induces a surface current on the target. A scattered wave from the target is produced by the surface current and propagates back to the observation point that coincides with the source point.

The target is assumed as a conducting cylinder with a cross-section expressed as

$$r = a[1 - \delta \cos 3(\theta - \phi)] \tag{1}$$

where a is the mean size of the target in which $a \ll \mathbf{r}_t$, δ is the concavity index, and ϕ is the rotation index.

Using the current generator Y_E and Green's function in free space $G_0(\mathbf{r} | \mathbf{r}')$, we can express the scattered wave as

$$u_s(\mathbf{r}) = \int_S d\mathbf{r}_1 \int_S d\mathbf{r}_2 [G_0(\mathbf{r} | \mathbf{r}_2) Y_E(\mathbf{r}_2 | \mathbf{r}_1) u_{in}(\mathbf{r}_1 | \mathbf{r}_t)] \quad (2)$$

where $u_{in}(\mathbf{r}_1 | \mathbf{r}_t)$ is expressed as

$$u_{in}(\mathbf{r}_1 | \mathbf{r}_t) = G_0(\mathbf{r}_1 | \mathbf{r}_t) \quad (3)$$

whose dimension coefficient is understood. Here, Y_E is the operator that transforms incident waves into surface currents on S and depends only on the scattering body [7–10]. The current generator can be expressed in terms of wave functions that satisfy Helmholtz equation and the radiation condition. That is, for E-wave incidence, the surface current is obtained as

$$\begin{aligned} & \int_S Y_E(\mathbf{r}_2 | \mathbf{r}_1) u_{in}(\mathbf{r}_1 | \mathbf{r}_t) d\mathbf{r}_1 \simeq \\ & \mathbf{\Phi}_M^*(\mathbf{r}_2) A_E^{-1} \int_S \ll \mathbf{\Phi}_M^T(\mathbf{r}_1), u_{in}(\mathbf{r}_1 | \mathbf{r}_t) \gg d\mathbf{r}_1 \end{aligned} \quad (4)$$

where

$$\begin{aligned} & \int_S \ll \mathbf{\Phi}_M^T(\mathbf{r}_1), u_{in}(\mathbf{r}_1 | \mathbf{r}_t) \gg d\mathbf{r}_1 \equiv \\ & \int_S \phi_m(\mathbf{r}_1) \frac{\partial u_{in}(\mathbf{r}_1 | \mathbf{r}_t)}{\partial n} - \frac{\partial \phi_m(\mathbf{r}_1)}{\partial n} u_{in}(\mathbf{r}_1 | \mathbf{r}_t) d\mathbf{r}_1 \end{aligned} \quad (5)$$

Above equation is sometimes called “reaction” named by Rumsey [22]. Here, the basis functions $\mathbf{\Phi}_M$ are called the modal functions and constitute the complete set of wave functions satisfying the Helmholtz equation in free space and the radiation condition; $\mathbf{\Phi}_M = [\phi_{-N}, \phi_{-N+1}, \dots, \phi_N]$, $M = 2N + 1$ is the total mode number, $\phi_m(\mathbf{r}) = H_m^{(1)}(kr) \exp(im\theta)$, and A_E is a positive definite Hermitian matrix given by

$$A_E = \begin{pmatrix} (\phi_{-N}, \phi_{-N}) & \dots & (\phi_{-N}, \phi_N) \\ \vdots & \ddots & \vdots \\ (\phi_N, \phi_{-N}) & \dots & (\phi_N, \phi_N) \end{pmatrix} \quad (6)$$

in which its m, n element is the inner product of ϕ_m and ϕ_n :

$$(\phi_m, \phi_n) \equiv \int_S \phi_m(\mathbf{r}) \phi_n^*(\mathbf{r}) d\mathbf{r} \quad (7)$$

The Y_E is proved to converge in the sense of mean on the true operator when $M \rightarrow \infty$. We can obtain the RCS σ as follows:

$$\sigma = \langle |u_s(\mathbf{r})|^2 \rangle \cdot k(4\pi z)^2 \quad (8)$$

The calculation of scattering data has been restricted to the interval $0.1 < ka < 30$. It is quite difficult to exceed this ka 's limit since larger ka requires so big M which consequently enlarges the calculation time dramatically.

In the physical-optics approximation (PO), the RCS is given by [10–13] which assumes zero surface current on the shadow region. The validity of (9) was confirmed experimentally by [23] and also theoretically by [24].

$$\sigma = k \left| \int_S n e^{-j2k\mathbf{r}_t \cdot \mathbf{r}'} d\mathbf{r}' \right|^2 \quad (9)$$

where n is the normal vector to the target surface in the outward direction.

3. NUMERICAL RESULTS

Here, RCS calculations for concave illumination region of concave-convex targets are presented in Figure 2. Using our exact method defined in (8), it is observed that the behavior of RCS is different from that one with convex illumination region that was shown in [7]. This difference is attributed to the contributions from complex saddle points that lie near the concave-to-convex transitions on the physical contour as has been described in [14]. The effect of target's curvature represented by δ is, therefore, limited on RCS in case of convex illumination region. On the other hand, δ has more influence on the waves scattered from concave region; as we perceive with big δ , the RCS increases with ka to a certain limit and then decreases in a stepwise manner. Such behavior can be explained as follows: as magnifying δ , the concavity of the incident area expands which in turn increases the effective illumination region. Therefore, the contributions from this region become sometimes in phase so they add up and sometimes out of phase so they cancel out with ka depending on the real and complex scattering rays directions and that leads to such up-down behavior with $\delta = 0.18, 0.2$. However, with smaller δ , the specular reflections reduce as a result of lowering the concavity slope of the effective illumination region. So in such case and with expanding ka , the illumination region is stretched and, accordingly, the scattering waves progress in same directions and be in phase so they add up and therefore RCS keeps increasing gradually with ka .

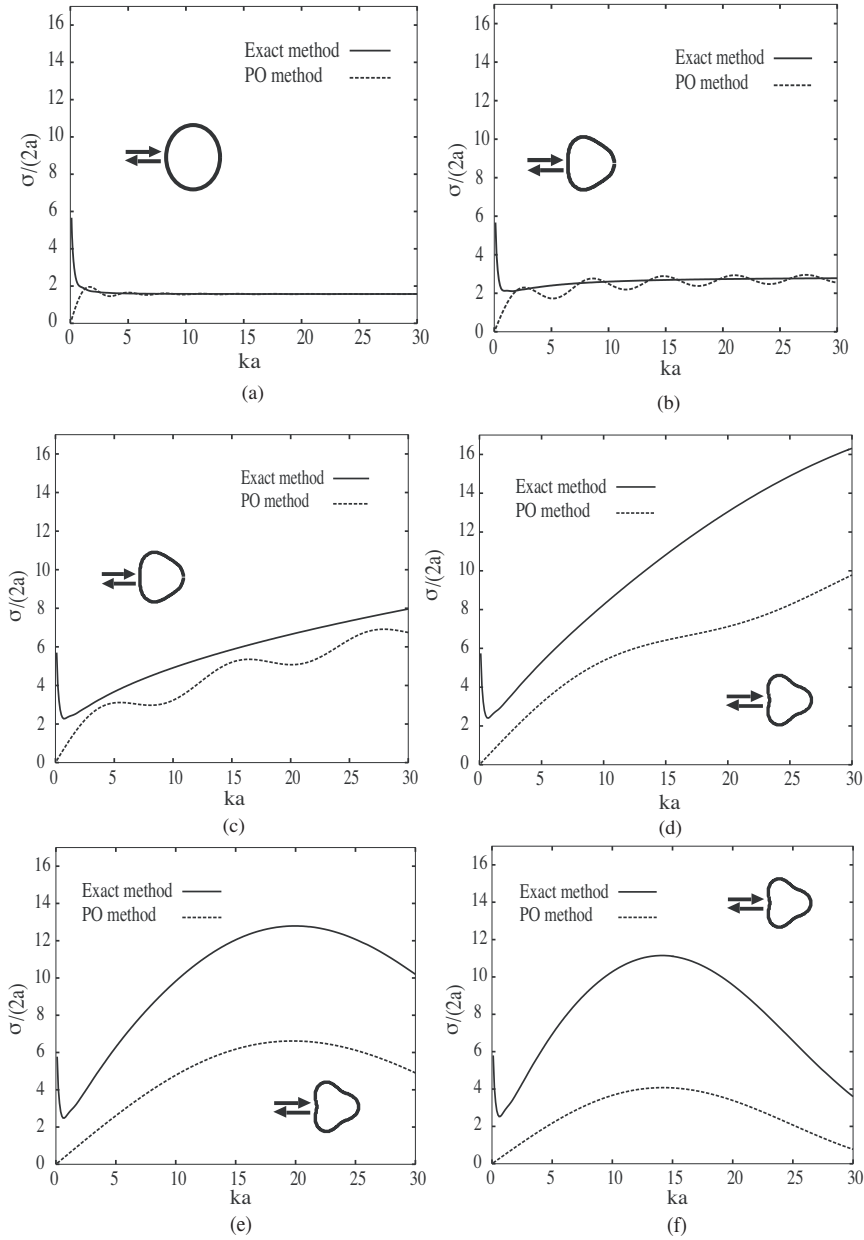


Figure 2. RCS vs. target size using exact method and PO method where (a) $\delta = 0$, (b) $\delta = 0.05$, (c) $\delta = 0.1$, (d) $\delta = 0.15$, (e) $\delta = 0.18$, (f) $\delta = 0.2$.

To verify the effect of the shadow region, we use PO method defined in (9) to estimate RCS. Numerical results for RCS behavior using our exact method are in good agreement with the approximate PO method apart from the magnitude. It is obvious that the magnitude of RCS with PO method deviates from our exact method especially with enlarging the concavity of the scatterer implemented by δ . This is attributed to the nonspecular contributions from the shadow region that includes as well those points in the vicinity of concave-to-convex inflection points on the scatterer surface as was pointed out in [9, 14, 15]. As well known, these contributions are not considered in the RCS estimate using PO method. In Figure 2(a), in the high frequency range, RCS performance completely agrees with that presented in our previous study in [7] where the target has circular cross section ($\delta = 0$). This is owing to having only one stationary point and the shadow region has no seeming effect on the scattering waves as a result of the lack in the vicinity of concave-convex inflection points. This proves that illuminating and scattered waves are subject to wavefront curvature [25].

4. CONCLUSION

The RCS of conducting targets with inflection points behaves in a way that can be explained as a result of the contributions from the effective illumination region in addition to the shadow region that includes the vicinity of concave-to-convex transitions on the scatterer surface. The nonspecular contributions interpret the effect of shadowed side on the scattering data compared to the calculation that considers the illumination region only as the case with physical optics method tested here on the same targets. All features in reference data for the RCS using our exact method have been discussed completely. Target's configuration including curvature and size is playing a primary role on the RCS especially for concave illumination region of partially convex targets.

ACKNOWLEDGMENT

This work was supported in part by National Science and Engineering Research Council of Canada (NSERC) under Grant 250299-02.

REFERENCES

1. Paddison, F. C., C. A. Shipley, A. L. Maffett, and M. H. Dawson, "Radar cross section of ships," *IEEE Trans. on Aerospace and*

- Electronic Systems*, Vol. AES-14, No. 1, 1978.
2. Jones, R. K. and T. H. Shumpert, "Surface currents and RCS of a spherical shell with a circular aperture," *IEEE Trans. Antennas Propagat.*, Vol. AP-28, No. 1, 128–132, 1980.
 3. Li, Y.-L., J.-Y. Huang, and M.-J. Wang, "Investigation of electromagnetic complex scattering for conductor target based on electromagnetic images method," *Progress In Electromagnetics Research*, PIER 81, 343–357, 2008.
 4. Cendes, Z. J. and P. Silvester, "Numerical solution of dielectric loaded waveguides: I. Finite-element analysis," *IEEE Trans. on Microwave Theory and Techniques*, Vol. 18, 1124–1131, 1970.
 5. Rao, S. M., D. R. Willton, and A. W. Glission, "Electromagnetic scattering by surface of arbitrary shape," *IEEE Trans. on Antennas and Propagation*, Vol. 30, 409–418, May 1982.
 6. Engheta, N., W. D. Murphy, V. Rokhlin, and M. S. Vassiliou, "The fast multipole method (FMM) for electromagnetic scattering problems," *IEEE Trans. Antennas Propagat.*, Vol. 40, No. 6, 634–641, 1992.
 7. El-Ocla, H. and M. Tateiba, "Backscattering enhancement for partially convex targets of large sizes in continuous random media for E-wave incidence," *Waves in Random Media*, Vol. 12, No. 3, 387–397, 2002.
 8. El-Ocla, H., "Backscattering from conducting targets in continuous random media for circular polarization," *Waves in Random and Complex Media*, Vol. 15, No. 1, 91–99, 2005.
 9. El-Ocla, H., "Laser backscattered from conducting targets of large sizes in continuous random media for E-wave polarization," *Journal of the Optical Society of America A*, Vol. 23, No. 8, 1908–1913, 2006.
 10. El-Ocla, H., "Backscattering enhancement analysis for targets in continuous random media based on wave polarization," *Waves in Random and Complex Media*, Vol. 18, No. 1, 13–25, 2008.
 11. Kerker, M., *The Scattering of Light and Other Electromagnetic Radiation*, Academic Press, New York, 1969.
 12. Howell, N. A. and G. S. Tsiang, "Computerized ray optics method of calculating average value radar cross section," *IEEE Trans. Antennas Propagat.*, Vol. AP-16, No. 5, 569–572, 1968.
 13. Meng, Z. Q. and M. Tateiba, "Radar cross sections of conducting elliptic cylinders embedded in strong continuous random media," *Waves in Random Media*, Vol. 6, 335–45, 1996.
 14. Ikuno, H. and L. B. Felsen, "Complex ray interpretation of

- reflection from concave-convex surface," *IEEE Trans. Antennas Propagat.*, Vol. 36, No. 9, 1260–1271, 1988.
15. Ikuno, H. and L. B. Felsen, "Complex rays in transient scattering from smooth targets with inflection points," *IEEE Trans. Antennas Propagat.*, Vol. 36, No. 9, 1272–1280, 1988.
 16. Crabtree, G. D., "A numerical quadrature technique for physical optics scattering analysis," *IEEE Trans. on Magnetics*, Vol. 27, No. 5, 4201–4294, 1991.
 17. Gordon, W. B., "High frequency approximations to the physical optics scattering integral," *IEEE Trans. Antennas Propagat.*, Vol. 42, No. 3, 427–433, 1994.
 18. Obelleiro-Basteiro, F., J. L. Rodriguez, and R. J. Burkholder, "An iterative physical optics approach for analyzing the electromagnetic scattering by large open-ended cavities," *IEEE Trans. Antennas Propagat.*, Vol. 43, No. 4, 356–361, 1995.
 19. Saeedfar, A. and K. Barkeshli, "Shape reconstruction of three-dimensional conducting curved plates using physical optics, NURBS modeling, and genetic algorithm," *IEEE Trans. Antennas Propagat.*, Vol. 54, No. 9, 2006.
 20. Adachi, S., "The nose-on echo area of axially symmetric thin bodies having sharp apices," Ohio State Univ., Columbus, OH, Res. Foundation, Rep. 951-I, AD240851, Mar. 1960. (Also, *Proc. IEEE*, Vol. 53, 1067–1068, Aug. 1965.)
 21. Adachi, S., A. Ohashi, and T. Uno, "Iterative radar target imaging based on modified extended physical optics method," *IEEE Trans. Antennas Propagat.*, Vol. 38, No. 6, 847–852, 1990.
 22. Rumsey, V. H., "Reaction concept in electromagnetic theory," *Physical Review*, Vol. 94, 1483–1491, 1954.
 23. Blore, W. E., "The radar cross section of ogives, double-backed cones, double-rounded cones and cone spheres," *IEEE Trans. Antennas Propagat.*, Vol. AP-12, No. 9, 582–590, 1964.
 24. De Wolf, A., "Radar reflectivity of metallic bodies of revolution," *IEEE Trans. Antennas Propagat.*, Vol. AP-17, No. 9, 665–667, 1969.
 25. Falconer, D., "Extrapolation of near-field RCS measurements to the far zone," *IEEE Trans. Antennas Propagat.*, Vol. 36, No. 6, 822–829, 1988.